

ATLAS: Adaptive Topology- and Load-Aware Scheduling

Jonathan Lutz, Charles J. Colbourn, and Violet R. Syrotiuk
CIDSE, Arizona State University, Tempe, AZ 85287-8809
Email: {jlutz, colbourn, syrotiuk}@asu.edu

Abstract—The largest strength of contention-based MAC protocols is simultaneously the largest weakness of their scheduled counterparts: the ability to adapt to changes in network conditions. For scheduling to be competitive in mobile wireless networks, continuous adaptation must be addressed. We propose ATLAS, an Adaptive Topology- and Load-Aware Scheduling protocol to address this problem. In ATLAS, each node computes its *persistence*, the fraction of time it is permitted to transmit, in a topology and load dependent manner. A distributed auction piggybacks offers and claims onto existing network traffic to compute a lexicographic max-min channel allocation. A node's persistence p is related to its allocation. Its schedule achieving p is updated where and when needed, without waiting for a frame boundary. We study how ATLAS adapts to controlled changes in topology and load. Our results show that ATLAS converges to most network changes in less than 0.1s, with about 20% relative error, scaling with network size. We further study ATLAS in more dynamic networks and show that it keeps up with topology changes, and load changes sufficient for TCP to sustain multi-hop flows, a struggle in IEEE 802.11 networks. The predictable performance of ATLAS supports the design of higher-layer services that inform, and are informed by, the underlying communication network.

Index Terms—Wireless networks, medium access control, adaptation.

I. INTRODUCTION

Despite the well known shortcomings of IEEE 801.11 and other contention-based MAC protocols for mobile wireless networks — such as probabilistic delay guarantees, severe short-term unfairness, and poor performance at high load — they remain the access method of choice. The primary reason is their ease in adapting to changes in network conditions, specifically to changes in topology and in load. The lack of timely adaptation is the most serious limitation facing scheduled MAC protocols. For scheduling to be competitive, continuous adaptation is required.

Topology-dependent approaches to adaptation in scheduling alternate a contention phase with a scheduled phase. In the contention phase, nodes exchange topology information used to compute a conflict-free schedule that is followed in the subsequent scheduled phase (see, as examples, [5], [36]). However, changes in topology and load do not always align with the phases of the algorithm resulting in a schedule that often lags behind the network state.

In contrast, the idea behind *topology-transparent* scheduling is to design schedules independent of the detailed network topology [4], [19]. Specifically, the schedules do not depend on the identity of a node's neighbours, but rather on *how many*

of them are transmitting. Even if a node's neighbours change, its schedule does not; if the number of neighbours does not exceed the designed bound then the schedule guarantees success. Though such schedules are robust to network conditions that deviate from the design parameters [31], because the schedules do not adapt, the technique remains a theoretical curiosity.

In contention-based schemes, such as IEEE 802.11, a node computes *implicitly* when to access the channel. We instead compute a node's *persistence* — the fraction of time it is permitted to transmit — *explicitly* in a way that tracks the current topology and load. To achieve this, we propose ATLAS, an Adaptive Topology- and Load-Aware Scheduling protocol. Channel allocation is a resource allocation problem where the demands correspond to transmitters, and the resources to receivers. The lexicographic max-min allocation to transmitters is the *TLA allocation* emphasizing that it is both *topology-* and *load-aware*. In ATLAS, a distributed auction runs *continuously*. It piggybacks offers and claims onto existing network traffic to compute the TLA allocation. Each node's schedule, achieving a persistence informed by its allocation, is updated whenever a change in topology or load results in a change in allocation. While the slots of the schedule are grouped into frames, this is done only to reduce the variance in delay [6]; there is no need to wait for a frame boundary to update the schedule. We study how ATLAS adapts to controlled changes in topology and load, measuring convergence time, relative error, and scalability. We also assess the ability of ATLAS to adapt in more dynamic network conditions.

To the best of our knowledge, ATLAS is the first scheduled MAC protocol able to adapt to changes in topology and load that is competitive with contention-based protocols in throughput and delay while realizing superior delay variance. It achieves this through the continuous computation of the TLA allocation, and updating the schedule on-the-fly. These updates occur only where and when needed. By not requiring phases of execution, ATLAS eliminates the complexity of, and lag inherent in, topology-dependent approaches. By not being dependent on the identity of neighbours, ATLAS shares the best of topology-transparent schemes yet overcomes its weakness. By not forcing updates to be frame synchronized, ATLAS shares the critical features of continuous adaptation with contention-based protocols.

As a result, ATLAS achieves predictable throughput and delay characteristics. Such characteristics and information about localized capacity at the MAC layer may be used to

arXiv:1305.4897v1 [cs.NI] 21 May 2013

inform higher layers, while end-to-end characteristics at higher layers may be used to inform the MAC layer. This may support the development of agile, higher performing protocols.

The sequel is organized as follows: §II defines a general resource allocation problem, provides a distributed algorithm to compute the lexicographic max-min allocation and proves its correctness. §III expresses channel allocation in terms of the resource allocation problem. The distributed algorithm computes the TLA allocation used in ATLAS. After describing the simulation set-up in §IV, §V studies how ATLAS adapts to controlled changes in topology and load, and to dynamic network conditions. In §VI, we discuss potential applications of the distributed algorithm with an emphasis of how ALTAS supports the design of higher-layer services that inform, and are informed by, the underlying communication network. Related work is described in §VII.

II. DISTRIBUTED RESOURCE ALLOCATION

We begin by defining a general resource allocation problem. Let R be a set of N resources with capacity $\mathbf{c} = (c_1, \dots, c_N)$. Let D be a set of M demands with magnitudes $\mathbf{w} = (w_1, \dots, w_M)$. Resource $j \in R$ is required by demands $D_j \subseteq D$. Demand $i \in D$ consumes capacity at all resources in $R_i \subseteq R$ simultaneously. The resource allocation $\mathbf{s} = (s_1, \dots, s_M)$, $s_i \geq 0$ defines the capacity reserved for the M demands. Resource allocation \mathbf{s} is *feasible* if $\sum_{i \in D_j} s_i \leq c_j$ for all $j \in R$ and $s_i \leq w_i$ for all $i \in D$. Demand $i \in D$ is *satisfied* if $s_i \geq w_i$. Resource $j \in R$ is *saturated* if $\sum_{i \in D_j} s_i \geq c_j$. Throughout, *capacity* refers to the magnitude of a resource.

Definition 1: [28] A feasible allocation \mathbf{s} is *lexicographically max-min* if, for every demand $i \in D$, either i is satisfied, or there exists a saturated resource j with $i \in D_j$ where $s_i = \max(s_k : k \in D_j)$.

We now describe a distributed algorithm to compute the lexicographic max-min allocation. In it, each resource is represented by an auctioneer and each demand by a bidder. Auctioneer j runs one auction to distribute capacity at resource j ; bidder i claims resources for demand i .

Bidder i knows w_i and maintains set R_i . Offers are stored in $\text{offers}[]$; $\text{offers}[j]$ holds the offer last received from auctioneer j . Bidder i constrains its *claim* to be no larger than w_i or the smallest offer from auctioneers in R_i ,

$$\text{claim} = \min(\{\text{offers}[j] : j \in R_i\}, w_i). \quad (1)$$

Auctioneer j knows c_j and maintains set D_j . Bidder claims are stored in $\text{claims}[]$; $\text{claims}[i]$ holds the claim last received from bidder i . Auctioneer j identifies set $D_j^* \subseteq D_j$ containing bidders with claims strictly smaller than its offer,

$$D_j^* = \{b : b \in D_j, \text{claims}[b] < \text{offer}\}. \quad (2)$$

Bidders in D_j^* are constrained elsewhere and cannot increase their claims in response to a larger offer from auctioneer j . Bidders in $D_j \setminus D_j^*$ are constrained by auction j . They may increase their claims in response to a larger offer. Resources left unclaimed by bidders in D_j^* ,

$$A_j = c_j - \left(\sum_{i \in D_j^*} \text{claims}[i] \right), \quad (3)$$

Algorithm 1 Bidder for Demand i .

```

1: upon initialization
2:    $R_i \leftarrow \emptyset$ 
3:    $w_i \leftarrow 0$ 
4:   UPDATECLAIM()
5: end upon
6: upon receiving a new demand magnitude  $w_i$ 
7:   UPDATECLAIM()
8: end upon
9: upon receiving offer from auctioneer  $j$ 
10:   $\text{offers}[j] \leftarrow \text{offer}$ 
11:  UPDATECLAIM()
12: end upon
13: upon bidder  $i$  joining auction  $j$ 
14:   $R_i \leftarrow R_i \cup j$ 
15:  UPDATECLAIM()
16: end upon
17: upon bidder  $i$  leaving auction  $j$ 
18:   $R_i \leftarrow R_i \setminus j$ 
19:  UPDATECLAIM()
20: end upon
21: procedure UPDATECLAIM()
22:   $\text{claim} \leftarrow \min(\{\text{offers}[j] : j \in R_i\} \cup w_i)$ 
23:  send claim to all auctions in  $R_i$ 
24: end procedure

```

are offered in equal portions to bidders in $D_j \setminus D_j^*$. If claims of all bidders in D_j are smaller than the offer (i.e., $D_j = D_j^*$), there are no bidders to share resources in A_j . The auctioneer sets its offer to A_j plus the largest claim, ensuring that any adjacent claim can be increased to consume resources in A_j :

$$\text{offer} = \begin{cases} A_j / |D_j \setminus D_j^*|, & \text{if } D_j \neq D_j^*, \\ A_j + \max(\text{claims}[i] : i \in D_j), & \text{otherwise.} \end{cases} \quad (4)$$

Alg. 1 and Alg. 2 describe actions taken by bidders and auctioneers in response to externally triggered events. Collectively, auctioneers and bidders know the inputs to the allocation problem. Each bidder i maintains w_i and R_i ; each auctioneer j maintains c_j and D_j . As we will see, bidder claims converge on the lexicographic max-min solution to the allocation problem; the claim of bidder i is s_i .

The correctness of Alg. 1 and Alg. 2 is established in two steps: Lemma 1 establishes forward progress on the number of auctioneers to have converged on their final offer. Theorem 1 employs Lemma 1 to show eventual convergence to the lexicographic max-min allocation. Let claim_i denote the claim of bidder i and offer_j the offer of auctioneer j . Assume that the resource allocation remains constant for the period of analysis, that bidder i knows R_i and w_i , and that auctioneer j knows D_j and c_j . Further assume communication between adjacent auctioneers and bidders is not delayed indefinitely. A claim or offer is *stable* if it has converged on its final value. Denote by A_{stable} the set of auctioneers whose offers (1) are stable and (2) remain the smallest among all offers.

Lemma 1: Suppose A_{stable} contains k auctioneers, $0 \leq k < N$. Then, within finite time, at least one auctioneer converges on the next smallest offer o_{\min} . Offers equal to o_{\min} are stable and remain smaller than all other offers not in A_{stable} .

Proof: Wait sufficient time for every bidder i to send a new claim to auctioneers in R_i and for every auctioneer j to send a new offer to bidders in D_j . Let o_{\min} be the smallest

Algorithm 2 Auctioneer for Resource j .

```

1: upon initialization
2:    $D_j \leftarrow \emptyset$ 
3:    $c_j \leftarrow 0$ 
4:   UPDATEOFFER()
5: end upon
6: upon receiving a new capacity of  $c_j$ 
7:   UPDATEOFFER()
8: end upon
9: upon receiving claim from bidder  $i$ 
10:   $claims[i] \leftarrow claim$ 
11:  UPDATEOFFER()
12: end upon
13: upon bidder  $i$  joining auction  $j$ 
14:   $D_j \leftarrow D_j \cup i$ 
15:  UPDATEOFFER()
16: end upon
17: upon bidder  $i$  leaving auction  $j$ 
18:   $D_j \leftarrow D_j \setminus i$ 
19:  UPDATEOFFER()
20: end upon
21: procedure UPDATEOFFER()
22:   $D_j^* \leftarrow \emptyset$ 
23:   $\mathcal{A}_j \leftarrow c_j$ 
24:   $done \leftarrow \text{False}$ 
25:  while ( $done = \text{False}$ ) do
26:    if ( $D_j^* = D_j$ ) then
27:       $done \leftarrow \text{True}$ 
28:       $offer \leftarrow \mathcal{A}_j + \max(\{claims[i] : i \in D_j\})$ 
29:    else
30:       $done \leftarrow \text{True}$ 
31:       $offer \leftarrow \mathcal{A}_j / |D_j \setminus D_j^*|$ 
32:      for all  $b \in \{D_j \setminus D_j^*\}$  do
33:        if ( $claims[b] < offer$ ) then
34:           $D_j^* \leftarrow D_j^* \cup b$ 
35:           $\mathcal{A}_j \leftarrow \mathcal{A}_j - claims[b]$ 
36:           $done \leftarrow \text{False}$ 
37:      send  $offer$  to all bidders in  $D_j$ 
38: end procedure

```

offer of an auctioneer not in A_{stable} . Assume to the contrary that $offer_x$ for some auctioneer $x \notin A_{\text{stable}}$ is the *first* to become smaller than o_{\min} . By Eq. 2 and 4, a decrease to $offer_x$ can only occur *after* a bidder y at auction x with $claim_y < offer_x$ increases its claim. By Eq. 1, $claim_y$ can increase only *after* its limiting constraint starts out smaller than $offer_x$ and increases. Constraints in the system smaller than $offer_x$ are maximum claims, offers from A_{stable} , and offers equal to o_{\min} . Maximum claims and offers from A_{stable} do not change, leaving some auctioneer x' with $offer_{x'} = o_{\min}$ as the only potential limiting constraint for $claim_y$. By Eq. 2 and 4, $offer_{x'}$ can increase only *after* one of its bidders y' reduces its claim to be smaller than $offer_{x'}$. By Eq. 1, $claim_{y'}$ can get smaller only *after* one of its auctioneers, say x'' , reduces its offer to be $offer_{x''} < o_{\min} = offer_{x'}$ contradicting the assumption that $offer_x$ is the *first* to get smaller than o_{\min} . Therefore, offers equal to o_{\min} remain smaller than offers not from A_{stable} .

By Eq. 2 and 4, any auctioneer j offering o_{\min} can change only after a bidder i at auction j with $claim_i \leq o_{\min}$ changes. By Eq. 1, $claim_i$ only changes if its limiting constraint changes. Potential limiting constraints include w_i , offers from A_{stable} , and offers equal to o_{\min} . These constraints are stable; therefore, offers equal to o_{\min} are stable. ■

Theorem 1: Bidders and auctioneers of Alg. 1 and Alg. 2

compute the lexicographic max-min allocation.

Proof: We apply Lemma 1 to show by induction that every auctioneer eventually computes a stable offer.

Base Case: Consider an allocation problem with arbitrary w_i, c_j, R_i , and D_j for $1 \leq i \leq M, 1 \leq j \leq N$. Let $|A_{\text{stable}}| = 0$. By Lemma 1, at least one auctioneer eventually converges on a smallest offer o_{\min} . Offers equal to o_{\min} are stable and remain smallest among all offers. Add auctioneers offering o_{\min} to A_{stable} so that $|A_{\text{stable}}| \geq 1$.

Inductive Step: Let $|A_{\text{stable}}| = k, 1 \leq k < N$. Then, by Lemma 1 a non-empty set of auctioneers A^+ with $A^+ \cap A_{\text{stable}} = \emptyset$ eventually converge on the next smallest offer. Offers from A^+ remain smaller than offers not from A^+ or A_{stable} and are stable. Add auctioneers in A^+ to A_{stable} so that $|A_{\text{stable}}| \geq k + 1$.

By the principle of mathematical induction, all auctioneers are eventually added to A_{stable} . Wait for auctioneers to send their offers to adjacent bidders. Bidder claims are now stable. By Eq. 1, bidder i is either satisfied with its claim ($claim_i = w_i$) or its claim is maximal at an auction in R_i . By Definition 1, the claims are lexicographic max-min. ■

III. CHANNEL ALLOCATION IN WIRELESS NETWORKS

The problem of channel allocation in wireless networks can be expressed in terms of the resource allocation problem in §II. In this context, transmitters correspond to the demands in D and receivers to the resources in R . Label transmitters $\{1, \dots, M\}$ and receivers $\{1, \dots, N\}$. Receiver j is in R_i if it is within transmission range of transmitter i . D_j contains the transmitters for which receiver j is within transmission range. Receiver j is *adjacent* to transmitter i if $j \in R_i$ and $i \in D_j$. The sets D_j and R_i capture the network topology. For load, w_i at bidder i is set to the percentage of slots required to support the demand at transmitter i . Receiver capacities are set to one targeting 100% channel allocation. The lexicographic max-min solution $s = (s_1, \dots, s_M)$ for a given topology and traffic load is the *TLA allocation*.

To apply the distributed algorithm to channel allocation, we integrate it into ATLAS, a simple MAC protocol for networks of homogeneous nodes, each equipped with a single wireless transceiver. In ATLAS, each node runs a bidder (Alg. 1) and an auctioneer (Alg. 2) continuously. Nodes notify their auctioneers and bidders of topology changes, *i.e.*, new and lost neighbours, maintaining sets R_i and D_j . Likewise, each node updates its bidder's demand magnitude to accurately reflect its traffic load. Offers and claims are embedded within the MAC header of all transmissions to be piggybacked on existing network traffic. A node's offer and claim are received by all single-hop neighbours reaching the bidders and auctioneers that need to know the offer and claim. In time, the bidder claims converge on the TLA allocation s .

The TLA allocation could be interpreted directly as a set of persistences in a p -persistent MAC. However, we achieve lower variation in delay by introducing the notion of a frame [6]. Specifically, ATLAS divides time into slots which are organized into frames of v slots. Node i operates at persistence $p_i = s_i$. At the start of every frame and upon any change to

p_i , node i computes $k_i = \lfloor p_i v \rfloor + 1$ with probability π_i and $k_i = \lfloor p_i v \rfloor$ with probability $1 - \pi_i$ where $\pi_i = p_i v - \lfloor p_i v \rfloor$. Node i constructs a transmission schedule of k_i slots selected uniformly at random from the v slots in the frame. Over many frames, $E[k_i]/v$ approaches p_i where $E[k_i]$ is the expectation for k_i . Each node's selection of persistence p_i is informed by the state of its bidder.

There are many implementation choices to be made in applying the distributed algorithm to channel allocation. We identify three to be evaluated further in simulation.

A. Lazy or Eager Persistences

At the heart of ATLAS is its use of the TLA allocation computed by the distributed algorithm. Here, we identify a lazy and an eager approach to deriving transmitter persistences from the state of the algorithm.

A lazy approach sets persistence p_i equal to the *claim* of bidder i . Once converged, p_i matches the TLA allocation interpreted as a persistence. There is a potential disadvantage with being lazy. For many applications, nodes cannot predict future demand for the channel; they can only estimate demand based on past events, *i.e.*, packet arrival rate or queue depth. As a consequence, w_i lags the true magnitude of the demand at node i . If w_i is the limiting constraint for the *claim* of bidder i , the lag affects both the *claim* and persistence p_i . The end result is a sluggish response to increases in demand with potential for degraded performance as is seen in the TCP throughput results of §V-F.

Alternatively, an eager approach sets transmitter persistences according to the offers of adjacent auctioneers rather than the claim of its bidder, breaking direct dependence on estimation of w_i . Each bidder computes $p_i = \min(\text{offers}[j] : j \in R_i)$. Under stable conditions a node's channel *occupancy*, the fraction of time it spends transmitting, matches its TLA allocation; its occupancy is limited by the availability of packets to transmit which is no larger than w_i , even when $p_i > w_i$. The motivation for selecting p_i according to auctioneer offers becomes apparent when demands are dynamic. Consider the case where the demand at node i starts out at zero and increases abruptly. If p_i is set equal to the *claim* at bidder i , p_i remains equal to zero until w_i catches up with the demand increase. If, on the other hand, p_i is set equal to the smallest offer, it is already non-zero — even before the demand increase is detected — resulting in faster response to demand increases. With improved responsiveness comes the risk of short term channel over-allocation. A sudden increase to a node's demand can result in an occupancy greater than what is reported to adjacent auctions through the bidder's *claim*. Such over-allocation is not resolved until the demand estimate w_i catches up with the true demand and the bidder updates its *claim* to reflect the increased channel occupancy.

B. Physical Layer or MAC Layer Receivers

A central objective of the TLA allocation is to ensure no receiver is overrun. In a wireless network, receivers can be defined in terms of physical layer or MAC layer communication. At the physical layer, every node with an active neighbour is a

receiver. At the MAC layer, packets are filtered by destination address; a node is only a receiver if one of its neighbours has MAC packets destined to it.

If the TLA allocation is defined in terms of MAC layer receivers, non-receiving nodes can disable their auctions. Disabled auctions no longer constrain bidder claims, allowing for a potentially higher channel allocation, but also slow detection of MAC receivers. A node identifies itself as a receiver upon receiving a packet, but its ability to do so is contingent on not too much contention. It only takes the reception of a single MAC packet to re-enable the auction.

C. Weighted or Non-Weighted Bidders

So far, we have described a MAC protocol where transmitters are represented by equally weighted bidders. For applications requiring multiple demands per transmitter, we propose the *weighted* TLA allocation which allows demands comprised of one or more *demand fragments*; the number of fragments accumulated into a demand is the demand's *weight*. Let γ_i denote the weight for demand i . Demand fragments in demand i have magnitude w_i/γ_i . The weighted TLA allocation defines the lexicographically max-min vector $u = (u_1, \dots, u_N)$ where u_i is the allocation to *each* demand fragment in demand i for a total allocation of $u_i \gamma_i$ to demand i .

The distributed algorithm can be extended to compute the weighted TLA allocation. Each bidder transmits its weight γ_i alongside its *claim*. Auctioneers record the weights of adjacent bidders in a *weights[]* array; *weights[i]* holds the weight for bidder i . Bidder i sets its claim to be no larger than the offer of any adjacent auctioneer and no larger than w_i/γ_i . Eq. 1 becomes $\text{claim} = \min(\{\text{offers}[j] : j \in R_i\}, w_i/\gamma_i)$. The auctioneer's calculation of \mathcal{A}_j is modified to subtract the weighted claims for all bidders $i \in D_j^*$ from c_j . Eq. 3 becomes $\mathcal{A}_j = c_j - \left(\sum_{i \in D_j^*} \text{claims}[i] \cdot \text{weights}[i]\right)$. Finally, the available channel is offered in equal portions to demand fragments at bidders in $D_j \setminus D_j^*$. Eq. 4 becomes

$$\text{offer} = \begin{cases} \mathcal{A}_j / \left(\sum_{i \in D_j \setminus D_j^*} \text{weights}[i]\right), & \text{if } D_j \neq D_j^*, \\ \mathcal{A}_j + \max(\text{claims}[i] : i \in D_j), & \text{otherwise.} \end{cases}$$

IV. SIMULATION SET-UP

We now describe details of the simulation used to produce the experimental results for ATLAS presented in §V. The configurations are chosen to evaluate the three implementation options outlined in §III: eager or lazy persistences, MAC or physical layer receivers, and unweighted or weighted bidders. Table I lists the four ATLAS configurations simulated. The *Nominal* configuration employs eager persistences, defines receivers in terms of MAC layer communication, and operates with unweighted bidders. The other three configurations differ from the nominal case by a single choice and are named accordingly: *Lazy Persistences*, *Physical Receivers*, and *Weighted Bidders*.

A. Minimum Persistence p_{\min}

A node can maintain a persistence of zero without impacting the communication requirements of its bidder. For auctioneers,

TABLE I
ATLAS CONFIGURATIONS SELECTED FOR SIMULATION.

Configuration Name	Eager (0) or Lazy (1) Persistences	MAC (0) or Physical (1) Receivers	Unweighted (0) or Weighted (1) Bidders
Nominal	0	0	0
Lazy Persistences	1	0	0
Physical Receivers	0	1	0
Weighted Bidders	0	0	1

a persistence of zero is problematic. If a receiver becomes overwhelmed by neighbouring transmitters, a non-zero persistence is needed to quiet the neighbours. To accomplish this, the node enforces a minimum persistence p_{\min} , creating dummy packets if necessary, whenever the sum of claims from adjacent bidders exceeds the auction capacity.

B. Overriding the TLA Allocation with p_{default}

There are two conditions where a node constrains its persistence to be no larger than p_{default} . The first is when the node has no neighbours. The TLA allocation permits an isolated node to consume 100% of the channel. But, the primary task of an isolated node is to discover new neighbours, a task made impossible if it is always transmitting. By constraining the persistence to be no larger than p_{default} , the isolated node has a chance to discover new neighbours.

The second time a node employs p_{default} is after the discovery of a new neighbour. It is possible for two or more nodes operating with large persistences to join a neighbourhood at about the same time. If the persistences are large enough, the channel can be overwhelmed, preventing the nodes from discovering each other. By limiting the persistence for a short time following the discovery of a neighbour, the number of transmissions on the channel is reduced, improving odds of successful neighbour discovery.

C. Adaptation to Topology Changes and t_{lostNbr}

Changes in network topology are detected externally to the distributed algorithm. In ATLAS, neighbour discovery is performed independently by each node. If a node hears from a new neighbour, then the node notifies its bidder of the new auction and its auctioneer of the new bidder.¹ Conversely, if a node has not heard from a neighbour in more than t_{lostNbr} seconds, it presumes the node is no longer a neighbour and informs its auctioneer and bidder accordingly.

D. Scenario Details

Unless otherwise noted, all four configurations run with $p_{\text{default}} = 0.05$, $t_{\text{lostNbr}} = 0.5\text{s}$, and $p_{\min} = 0.01$. The selection of p_{default} and t_{lostNbr} are justified later in Fig. 3, 9a, and 9b. The selection of p_{\min} is based on [26]. Frames contain $v = 100$ slots of length $800\mu\text{s}$ (1100 bytes per slot).

Simulations are run using the ns-2 simulator [27]. Each wireless node is equipped with a single unicast transceiver and omni-directional antenna whose physical properties match

those of the 914 MHz Lucent WaveLAN DSS unicast radios. The data rate for all simulations is 11 Mbps. The transmission and carrier sense ranges are 250m.

Each simulation runs a network scenario composed of a randomly generated topology and a randomly generated traffic load. Unless specified otherwise, topologies contain 50 randomly placed nodes constrained to a 300m by 1500m area. With the exception of the multi-hop TCP flows in §V-F, each traffic load consists of single-hop constant rate traffic. Four traffic loads are simulated: 20% of nodes loaded with small demands (75 ± 50 pkts/s), 80% of nodes loaded with small demands, 20% of nodes loaded with large demands (500 ± 50 pkts/s), and 80% of nodes loaded with large demands. Nodes to be loaded with traffic are selected at random and the demand magnitudes are selected uniformly at random from the specified range. The packet destination is dynamically selected from the set of neighbouring nodes as the packet is passed down to the MAC layer. For the Weighted Bidders configuration, each demand is assigned a random integer weight between one and five. Combined with the random placement of nodes and the addition of mobility, these four traffic loads enable simulation of a wide variety of network conditions.

Traffic is generated by ns-2 Constant Bit Rate (CBR) generators; UDP provides transport layer services; packets are 900 bytes in length, leaving room in each slot for header bytes and a MAC layer acknowledgement. Unacknowledged MAC packets are retransmitted up to ten times before they are dropped by the sender.

E. Offer, Claim, and Weight Encoding

Offers and claims are encoded using eight bits to support a total of 256 unique persistences uniformly distributed between 0 and 1; the error in the representation does not exceed 0.004. Sixteen unique weights (requiring a four-bit representation) may be sufficient for many applications. Adding an offer, claim, and weight to the data packet and acknowledgement of each transmission brings the total communication overhead to five bytes per packet. For the slot size and data rate simulated in §V, the communication overhead is 0.46%.

F. Relative Error

A metric of interest is the average relative error for a node's persistence with respect to the TLA allocation. Error is reported in two parts: relative excess persistence error and relative deficit persistence error. Errors are measured per node over 0.08s consecutive intervals in time (equal to the length of one MAC frame). Let $\rho = (\rho_1, \dots, \rho_n)$ be a vector of n persistence measurements; ρ can contain measurements for one or more nodes. Each measurement ρ_i is associated with a node and time interval during which the TLA allocation defines a target persistence τ_i . The excess and deficit errors (ϵ_i^+ and ϵ_i^- , respectively) for persistence measurement ρ_i are $\epsilon_i^+ = \rho_i - \tau_i$ and $\epsilon_i^- = 0$ if $\rho_i > \tau_i$, and $\epsilon_i^+ = 0$ and $\epsilon_i^- = \tau_i - \rho_i$ otherwise. The relative errors are $\eta_i^+ = \epsilon_i^+ / \tau_i$ and $\eta_i^- = \epsilon_i^- / \tau_i$. Our intent is to compute the average relative excess error and average relative deficit

¹We implicitly assume a symmetric hearing matrix.

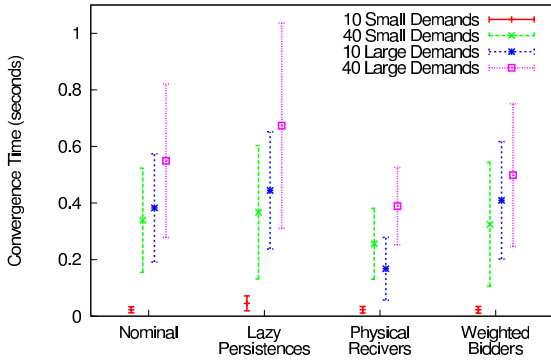


Fig. 1. Convergence time following network initialization.

error for a given sample set of persistence measurements. The relative errors are ratios, requiring use of the geometric rather than arithmetic mean. But, the errors η_i^+ and η_i^- are often zero, preventing direct use of their mean.² Instead, we convert errors into accuracies eliminating zeros from the data set for a more meaningful geometric average. The average relative accuracies are converted back to relative errors. Specifically, the expectation for excess relative persistence error is

$$E[\eta_i^+] = \left(\prod_{1 \leq i \leq n} (\eta_i + 1) \right)^{1/n} - 1$$

and the expectation for relative deficit persistence error is

$$E[\eta_i^-] = 1 - \left(\prod_{1 \leq i \leq n} (1 - \eta_i) \right)^{1/n}$$

V. EVALUATION OF ATLAS

The results in this section answer four questions concerning the ATLAS MAC protocol: How quickly does the protocol converge on the TLA allocation? Does it scale to larger networks? Can it keep up with changes in a mobile network? And, can it adapt to the needs of multi-hop traffic flows? Results of IEEE 802.11 are included as a common, well known point of reference to assist interpretation. In ATLAS, the upper network layers inform the MAC layer, providing traffic demands to the distributed algorithm. However, it is also possible for ATLAS to inform the decisions made at the upper layers; see §VI.

A. Convergence after Network Initialization

Fig. 1 reports average convergence times for all four configurations of ATLAS. Error bars denote the arithmetic standard deviation from the mean for each sample set. Convergence is measured from network initialization (time = 0) to the time the distributed algorithm converges on the TLA allocation. Times are collected from simulations of 1000 network scenarios simulated four times each, once per configuration. Each scenario consists of a randomly generated topology and traffic load; there are 250 scenarios for each traffic load.

The Physical Receivers configuration converges fastest in less than 0.4s on average for networks with 40 large demands and faster for other traffic loads. It is the only configuration to

enable all auctions unconditionally. The extra step of detecting MAC receivers slows convergence. The Lazy Persistences configuration is the slowest with an average convergence time of 0.67s for networks with 40 large demands. The strict limit on persistences enforced by this configuration compared to the other configuration slows convergence.

Fig. 2a shows average excess and deficit relative persistence errors for all four configurations. The averages are computed over measurements taken at nodes with a non-zero TLA allocation and only during convergence. Nodes are observed to operate within approximately 20% of their TLA allocation regardless of configuration. Deficit errors are larger than excess errors reflecting a tendency to converge from below, rather than above, the TLA allocation.

Fig. 2b plots total relative persistence error — deficit plus excess persistence error — against convergence time for the Nominal configuration. Each data point reflects the convergence time (x -coordinate) and total relative persistence error (y -coordinate) for one simulation. The data shows relative persistence error to be fairly consistent from network to network with a maximum observed error of 27%.

Fig. 3 reports convergence time for the Nominal configuration with different default persistences. Convergence is measured for simulations of 1000 randomly generated network scenarios, 250 of each traffic load. The scenarios are simulated eight times each, once per default persistence: 0.001, 0.005, 0.01, 0.05, 0.1, 0.2, 0.3, and 0.4. Small default persistences ($p_{\text{default}} \leq 0.01$) limit a node's ability to communicate during neighbour discovery, slowing convergence. Large default persistences ($p_{\text{default}} \geq 0.3$) permit nodes to transmit with large persistences before they discover their neighbours. In networks with 40 of 50 nodes loaded with large demands, the large persistences can overwhelm the channel preventing neighbour discovery and delaying convergence. The distributed algorithm is robust to the selection of p_{default} with a suitable range of [0.05–0.2]. For the remaining simulations, p_{default} is set to 0.05.

B. Convergence after a Change in Demand

Fig. 4 reports convergence times and relative persistence errors for the Nominal configuration following a change to a single demand magnitude. Four types of demand increase are simulated: a new small demand, a new large demand, a small demand increase, and a large demand increase. New demands start with magnitude zero and change to 75 ± 50 pkts/s for small demands and to 500 ± 50 pkts/s for large demands. Both small and large demand increases start at 75 ± 50 pkts/s and change to 150 ± 50 pkts/s for small increases and to 500 ± 50 pkts/s for large increases. Similarly, four types of demand decrease are simulated. Removed small demands and removed large demands start at 75 ± 50 pkts/s and at 500 ± 50 pkts/s respectively; both change to zero. Small demand decreases start at 150 ± 50 pkts/s and large demand decreases start at 500 ± 50 pkts/s; both change to 75 ± 50 pkts/s. The eight demand change types are simulated under the four traffic loads. The network is allowed to converge on the initial TLA allocation prior to the demand change. Convergence times and error measurements are taken from simulations of 8000

²The geometric mean of any data set containing zero is zero.

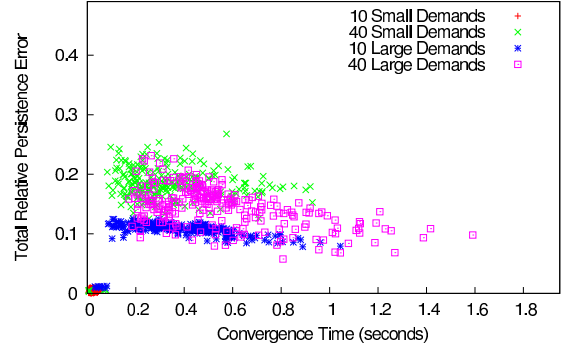
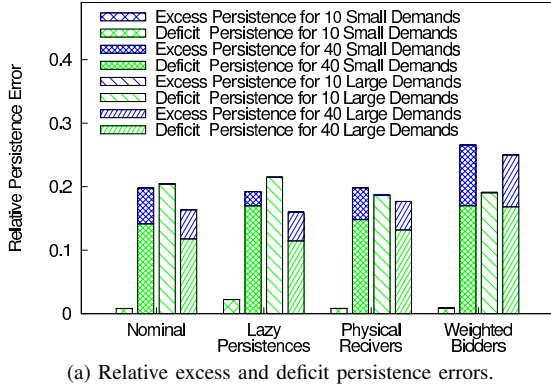


Fig. 2. Relative persistence error for ATLAS.

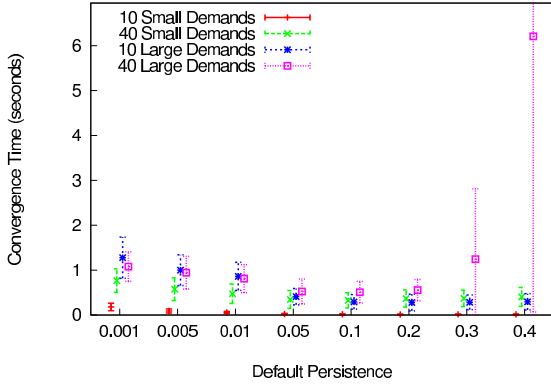


Fig. 3. Convergence times when run with varying default persistences.

randomly generated network scenarios, 250 for each of the 32 demand change and traffic load combinations.

Fig. 4a and 4c report convergence times measured from the time of the demand change to the time of convergence on the new TLA allocation. The largest convergence times of approximately 0.175s are found in networks loaded with 40 demands involving new or removed demands. The average convergence time for the other scenarios is 0.125s or smaller. Fig. 4b and Fig. 4d show relative persistence errors measured during convergence at nodes whose TLA allocation are affected by the demand change. Persistences are observed to be within 10% of the TLA allocation.

C. Convergence after a Change in Topology

Fig. 5 reports convergence time and relative persistence error following two types of topology change: the creation of a link and the removal of a link between a pair of nodes. Simulations are run on 2000 randomly generated network scenarios, 250 for each topology change type and traffic load combination. Networks that lose a link are simulated once per neighbour timeout t_{lostNbr} of 0.5s, 2.0s and 5.0s.

Network topologies are generated as follows. A first node is placed at a random location in the simulation area. A random point (x, y) is selected inside the simulation area and on the perimeter of the node's transmission range. For topologies gaining a link, a second node is placed near point (x, y) but just *outside* the transmission range of the first node with a

trajectory *toward* the first node. For topologies losing a link, the second node is placed near point (x, y) but just *inside* the transmission range of the first node with a trajectory *away* from the first node. The remaining 48 nodes are placed at random locations in the simulation area. The distance travelled by the second node is tightly constrained to avoid unintentional topology changes. In the event that a scenario is generated with more than one topology change, data collected from the scenario is not accumulated into the reported results.

The expectation for convergence time following the addition of a new link is 0.025s. The time required to converge after the removal of a link is dominated by the value selected for the neighbour timeout. For $t_{\text{lostNbr}} = 0.5$, convergence is reached in less than 0.13s on average. During convergence, nodes affected by the topology change are observed to operate within 4% of their TLA allocation on average.

These numbers are striking. The small convergence times stem from a counterintuitive feature of the TLA allocation: the majority of topology changes do not affect the TLA allocation. A new link only has an effect if the link connects a bidder with an auction that lacks the capacity to support the bidder's claim. Even in heavily loaded networks, many auctions have spare capacity to support a new bidder. For these scenarios, convergence is instantaneous.

D. Scalability to Large Networks

We now turn to results demonstrating ATLAS's ability to support large networks. We simulate 10 network sizes with the x -dimension ranging from 600m (2.4 hops) to 6000m (24 hops) in 600m increments; the y -dimension is held constant at 300m. The number of nodes is selected to keep the average neighbourhood density constant across all network sizes. Fig. 6 reports convergence times for four thousand randomly generated network scenarios, 100 of each traffic load and network size combination. ATLAS's ability to scale to large networks is striking. In networks spanning 24 hops, convergence is reached in an average of 0.89s, a mere 40% increase compared to networks spanning 4.8 hops.

The impressive convergence times, particularly those of networks spanning 12 or more hops, suggest that convergence happens locally, allowing distant neighbourhoods to converge in parallel. The local behaviour is captured in Fig. 7 which

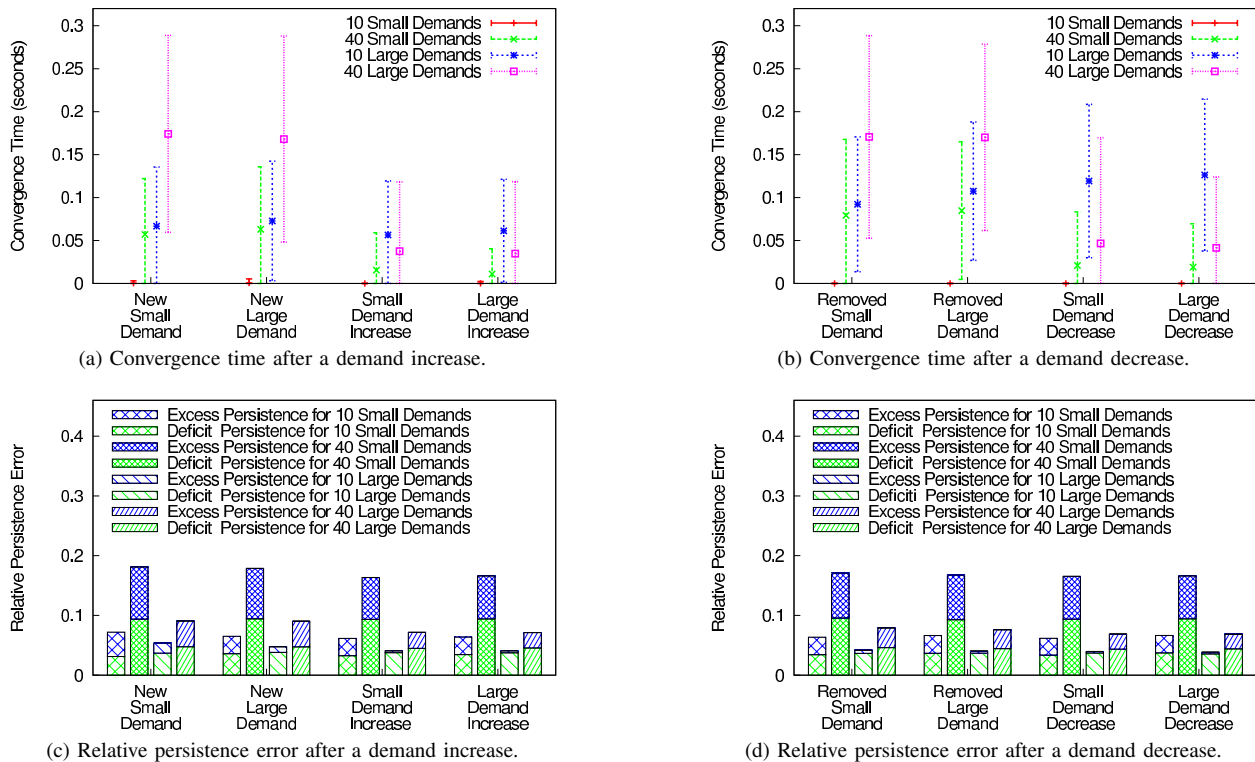


Fig. 4. Convergence time and relative persistence error during convergence following a single demand change.

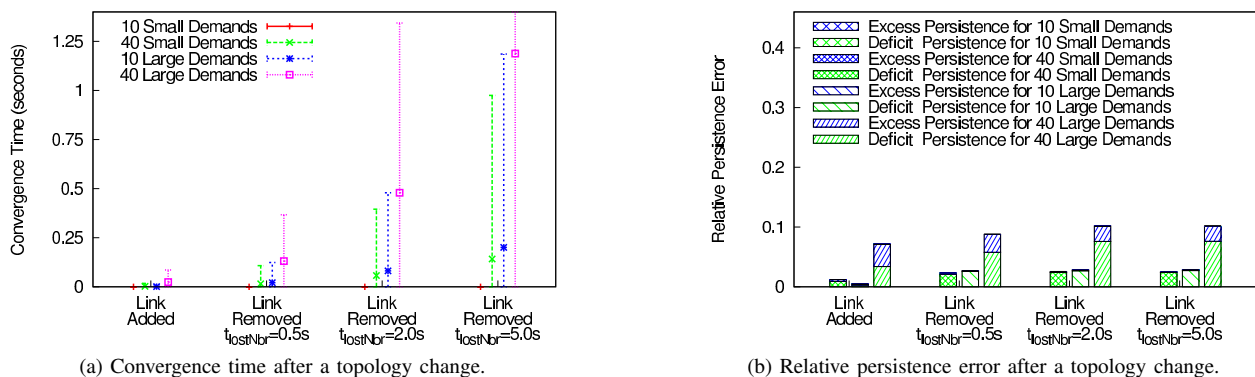


Fig. 5. Convergence time and relative persistence error following a single topology change.

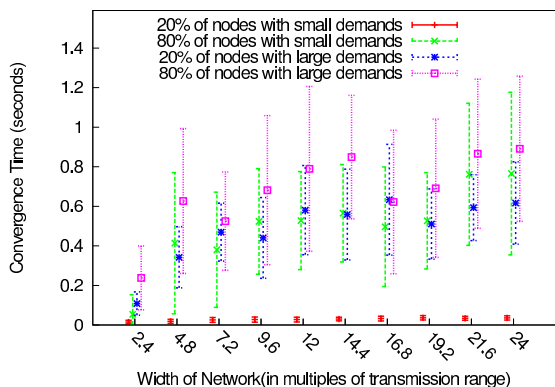


Fig. 6. Convergence times as the width of the network grows.

reports the expectation for distance between a network change and a node whose bidder changes its claim during convergence to the new TLA allocation. Distances are reported in hops. A node that changes its demand or gains/loses a neighbour has distance zero. Neighbours of this node have distance one, and so on. Range of impact is reported for six types of change: a new small demand, a new large demand, a removed small demand, a removed large demand, a removed link, and an added link. Each type of change is simulated in 1000 randomly generated network scenarios, 250 of each traffic load. The range of impact is less than 1.75 hops on average.

E. Performance with Node Mobility

§V-C addresses the robustness of ATLAS to single topology changes (*i.e.*, new and broken links). We now turn to evaluate

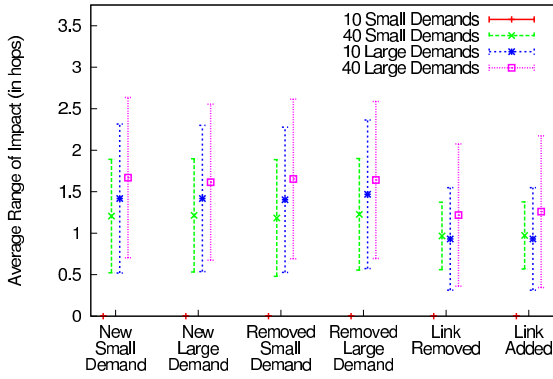


Fig. 7. Average range of impact (in hops) for a demand or topology change.

its performance in networks with continuous mobility which may not have the opportunity to fully converge on the TLA allocation. It does not make sense to report convergence times; instead, we focus on relative persistence error, total MAC throughput, and packet delay.

Fig. 8a reports persistence error for node speeds ranging from 0 m/s to 120 m/s with 200 random scenarios simulated for each node speed, 50 of each traffic load. Node movements are generated using the steady-state mobility model generator of [17] with a pause time of zero. Simulations are run for 20s. As node speeds increase, so do deficit persistence errors. The larger deficit errors are an artifact of lost neighbour detection which is delayed by up to $t_{\text{lostNbr}} = 0.5\text{s}$ for these simulations. As a result, nodes tend to think their neighbourhoods are more crowded than they are, a tendency that gets worse as node speeds increase. In terms of the distributed algorithm, auctioneers and bidders unnecessarily constrain their offers and claims to accommodate lost neighbours.

The deficit persistences translate to degraded throughput. Fig. 8b reports total MAC throughput for the simulations of Fig. 8a. Even with node speeds of 120 m/s where a node travels its transmission range in just over two seconds, throughput degrades modestly, decreasing by less than 20% when compared to networks without mobility.

Fig. 9 shows that a large t_{lostNbr} exacerbates deficit persistence error and further degrades throughput. Data is collected from 200 random scenarios, 50 of each traffic load. Each scenario is simulated five times with neighbour timeouts ranging from 0.1s to 15.0s. Node speeds are fixed at 30 m/s. Degraded performance is observed for large timeouts, $t_{\text{lostNbr}} \geq 0.5\text{s}$, but also for small timeouts, $t_{\text{lostNbr}} = 0.1\text{s}$. In networks loaded with 10 large demands, $t_{\text{lostNbr}} = 0.1\text{s}$ causes nodes to falsely identify lost neighbours that must be rediscovered at the cost of limiting persistences to p_{default} . The remaining simulations are run with $t_{\text{lostNbr}} = 0.5\text{s}$.

Fig. 10 reports packet delay for ATLAS and IEEE 802.11 for the 200 network scenarios of Fig. 8 with node speeds equal to 30 m/s. IEEE 802.11 is configured with a maximum packet retry count of seven for RTS, CTS, and ACKs and four for data packets [15]. The slot length is set to $20\mu\text{s}$; the minimum and maximum contention window sizes are 32 and 1024 slots, respectively. Each point in the scatter plot reports the average packet delay (x -coordinate) and variation in packet delay (y -

coordinate) for a single node. The largest reported average delay is 0.047s for ATLAS and 0.058s for IEEE 802.11. The largest reported variation in delay for ATLAS is 0.0016s^2 , just 3.6% of the 0.0444s^2 reported for IEEE 802.11.

F. Multi-hop TCP Flows

To this point, we have used MAC layer traffic to simulate a diverse set of network scenarios. We now turn to evaluate the performance of ATLAS using multi-hop TCP flows. To accommodate the dynamic nature of these flows, each node estimates its own demand by monitoring queue behaviour. Demand is estimated as the sum of two parts: $w_{\text{enqueue}} + w_{\text{level}}$. The percentage of channel required to keep up with the current enqueue packet rate is $w_{\text{enqueue}} = (\text{packet enqueue rate}) \cdot (\text{slot length})$ where the packet enqueue rate is computed from the previous 0.1s of enqueue history. The percentage of channel required to transmit all packets in the queue within 0.2s (i.e., 25 slots) is $w_{\text{level}} = [(\# \text{ packets in queue}) / 0.02\text{s}] \cdot (\text{slot length})$.

To avoid cross-layer interactions between the MAC and routing protocols, Dijkstra's shortest path algorithm [33] using accurate knowledge of the global topology computes the next hop address for all packet transmissions.

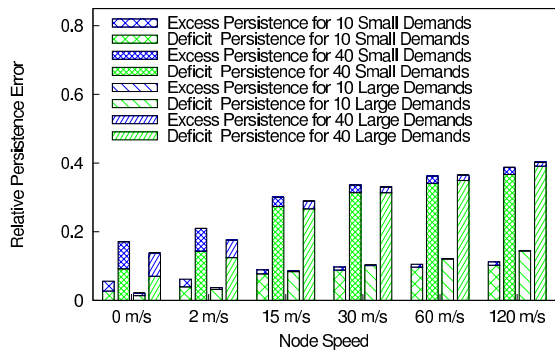
We simulate TCP traffic on five MAC protocols: the four configurations of ATLAS and IEEE 802.11. The configurations of ATLAS implement $p_{\text{default}} = 0.05$, $t_{\text{lostNbr}} = 0.5\text{s}$, and $p_{\text{min}} = 0.01$. IEEE 802.11 parameters match those described in §V-E. Each node dynamically sets its bidder weight to one or the number of outgoing TCP flows it services, whichever is larger.

FTP agents (bundled with `ns-2`) emulate transfer of infinite size files to create flows with throughput limited only by the performance of the network. Transfers start at time zero and run for 20s. Nodes are statically placed at random locations in a 300m by 1200m simulation area. The source and destination nodes for each FTP file transfer are selected at random. The majority of paths have five or fewer hops.

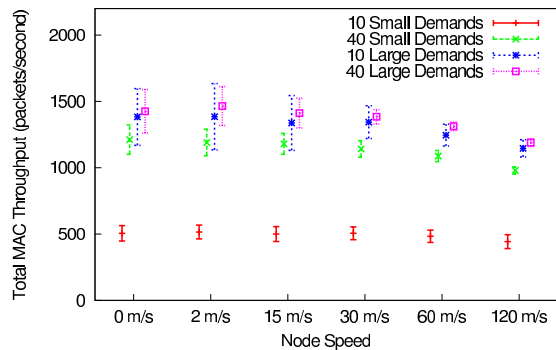
Each FTP transfer is transported over TCP Reno (bundled with `ns-2`) configured for selective acknowledgements, the extensions of RFC 1323 [1], and 900 byte TCP segments. The return ACKs are not combined with each other or with other data packets. Consequently, the transmission of a single 40-byte TCP ACK consumes an entire transmission slot in ATLAS. The maximum congestion window size is four packets to avoid the large delays caused by excessive queuing nodes along multi-hop paths [21], [22].

Network scenarios are simulated for three traffic loads: networks with two, eight, and 25 TCP flows. The number of replicates per traffic load are chosen so that 3000 TCP flows are simulated for each. Fifteen hundred scenarios are simulated with two TCP flows, 375 with eight TCP flows, and 120 with 25 TCP flows. Each scenario is simulated five times: once with IEEE 802.11 and once per ATLAS configuration.

The 15 sub-plots in Fig. 11 report on a subset of flows showing the percentage of flows (y -axis) achieving a minimum throughput (x -axis). The plots contain curves for all five MAC protocols. Plots in the left, center, and right columns report on flows from simulations of two, eight, and 25 flows,

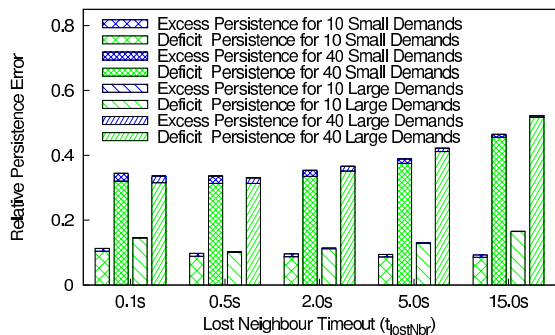


(a) Relative persistence error.

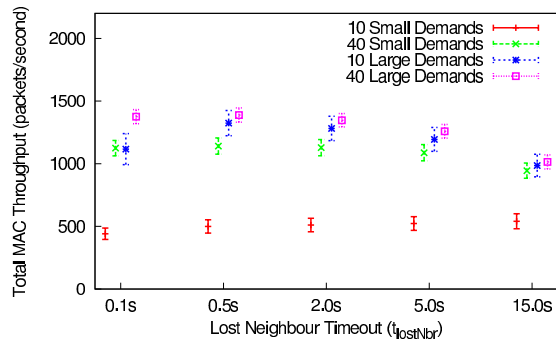


(b) Total MAC throughput.

Fig. 8. Relative persistence error and total MAC throughput for varying levels of node mobility.



(a) Relative persistence error.



(b) Total MAC throughput.

Fig. 9. Relative persistence error and total MAC throughput for varying neighbour timeouts.

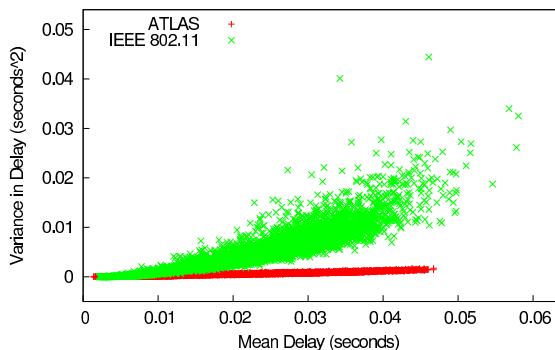


Fig. 10. Delays for ATLAS and IEEE 802.11.

respectively. The plots in the top row report on flows with five and fewer hops. Plots in the second, third, and fourth rows report on 1-hop, 2-hop, and 3-hop flows, respectively. Plots in the fifth row report on 4- and 5-hop flows.

The distinguishing characteristics of the three unweighted ATLAS configurations are seen in the throughput curves for networks with two flows. These networks are loaded lightly enough for the disabled auctions (at non-receiver nodes) to make a difference in the allocation, improving throughput for 2- and 4-hop flows. Networks with two flows also demonstrate how the longer initial packet delays of the Lazy Persistences configuration increase round trip time for 3-, 4-, and 5-hop flows, preventing TCP from maximizing its contention window and achieving its best throughput.

The Weighted Bidders configuration performs well for multi-hop flows in networks with eight and 25 flows by allocating more to multi-hop flows at the expense of single-hop flows. Because one-hop flows tend to achieve higher throughput, the configuration maintains a tighter variation in flow throughputs as signified by the steeper slope of the Weighted Bidders curve in the top right plot of Fig. 11.

Regardless of configuration, ATLAS surpasses IEEE 802.11 in support of concurrent multi-hop flows. The interaction between the IEEE 802.11 back-off algorithm and TCP's congestion control is well known [11]. In testbed experiments, a single TCP flow with no competition has difficulty reaching a destination four hops away [22]. Our simulations corroborate these findings with nearly 50% of the 4- and 5-hop flows reporting a throughput of zero. For networks with 25 demands, greater than 75% of 2-hop flows are non-functional; 3-, 4-, and 5-hop flows are almost completely shut out. The throughput of ATLAS is achieved in spite of channel wasted transmitting 40 byte TCP ACKs in their own slots. An intelligent packing of TCP ACKs may improve performance further.

VI. DISCUSSION

In this section we discuss strengths of ATLAS and suggest other potential applications of the distributed algorithm.

A. Improved Reliable Transport

TCP is known to perform poorly in wireless networks where signal fading and channel contention are frequent causes

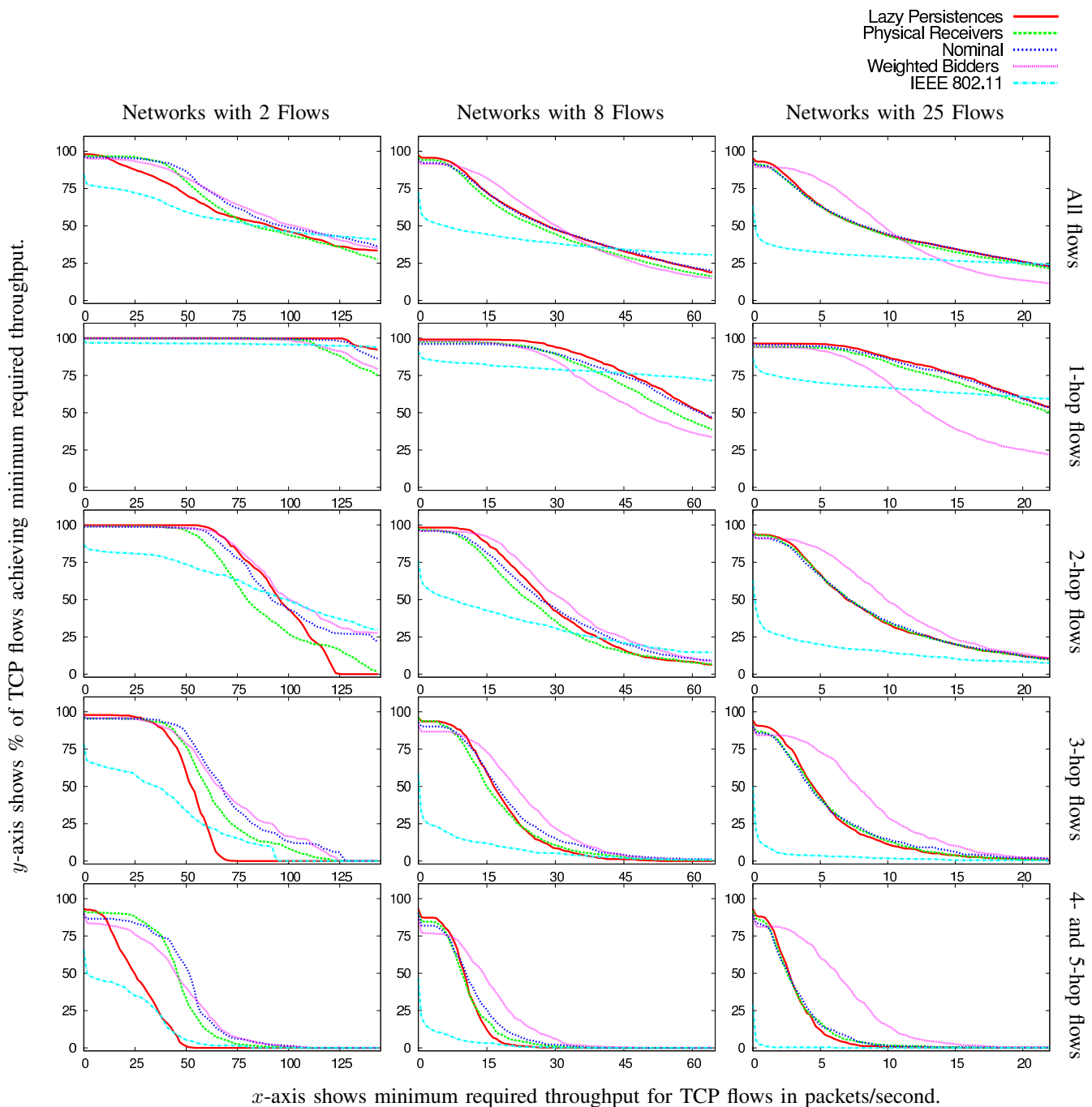


Fig. 11. Percent of TCP flows achieving a minimum throughput.

of packet loss [23]. Standard TCP assumes loss is due to congestion and responds by reducing its contention window size to limit the number of packets in the network. TCP's congestion control algorithm is further confused by cross-layer interactions with binary exponential back-off (BEB) employed by IEEE 802.11 [11]. BEB tends toward short term unfairness at the MAC layer allowing a single node to capture the channel at the expense of its neighbours [3], [13] causing high variation in packet delay and making it difficult for TCP to estimate round-trip delay. Multiple extraneous packet timeouts can cause TCP to back-off exponentially retransmitting packets as

infrequently as once per second [35].

Many modifications have been proposed to improve performance of TCP over wireless networks [23]; common approaches are detection of packet loss (differentiating it from congestion) and improved estimation of round trip time. An alternative is to minimize packet loss and control variation in packet delay at the MAC layer. ATLAS demonstrates a remarkable ability to control variation in delay (Fig. 10) enabling TCP to reliably support 3-, 4-, and 5-hop flows over heavily loaded networks (Fig. 11).

B. Robust to Selection of Configurable Parameters

ATLAS has three configurable parameters: p_{default} , t_{lostNbr} , and p_{min} . Based on our simulations, $[0.01\text{--}0.2]$ is an acceptable range for p_{default} (Fig. 3) and $[0.1\text{s--}2\text{s}]$ is an acceptable range for t_{lostNbr} (Figs. 9a, 9b). Selection of p_{min} is explored in [26] for a MAC that enforces a minimum persistence at all nodes and at all times; $p_{\text{min}} \geq 0.1$ is found to provide sufficient communication between auctioneers and bidders. As minimum persistence is increased, MAC throughput declines moderately for dense networks lightly loaded with a few large demands. The throughput decline is less pronounced for ATLAS because p_{min} is employed temporarily and only at nodes whose auction has become over-allocated.

C. Dynamic Selection of Auction Capacity

ATLAS targets 100% channel allocation by setting auction capacities to one. Although simulation results show this to be an adequate choice, it is not immediately clear whether performance can be improved by under-allocating or over-allocating the channel. Indeed, optimal auction capacities (however optimal is defined) are dependent on network topology and quality of the communication channel. We leave a thorough analysis of auction capacity selection to future work, pointing out here that the distributed algorithm adapts continuously to support dynamic selection of the auction capacities.

D. Potential Applications for the Distributed Algorithm

The weighted TLA allocation opens doors for several potential uses. In the simulations of §V-F, a bidder's weight is set according to the number of flows serviced by its host node. It may be desirable to set weights according to queue levels, demand magnitudes, neighbourhood sizes, node betweenness [8], distance from a point of interest (*i.e.*, an access point or a common sink), position in a multicast/broadcast tree, or path hop count. The key observation is that the distributed algorithm maintains flexibility by allowing nodes to define bidder weights arbitrarily to suit the needs of the network.

While computation of persistences continuously is the primary motivation for this work, the distributed algorithm is not limited to this purpose. Indeed, the algorithm provides a distributed method for computing the lexicographic max-min solution to any resource allocation problem and is, therefore, applicable to many areas of computer science and engineering. We overview several potential applications in the area of wireless networks.

Consider the Physical Receivers configuration with node demands set to one. The resulting allocation is independent of actions taken by the upper network layers and, therefore, can inform decisions made by those layers. The resulting allocation also serves as a measure of potential network congestion—small allocations are assigned in dense neighbourhoods containing many potentially active neighbours. The routing protocol can use the allocation to adjust link costs, enabling the discovery of faster, although possibly longer, routes around congestion.

An intriguing application is the implementation of differentiated service at the MAC layer. IEEE 802.11e [16] enhances

the distributed coordination function by implementing four access categories; from lowest to highest priority they are Background, Best Effort, Video, and Voice. Four instances of the back-off algorithm are run, one per access category, each with its own queue. The probability of transmission of each access category is manipulated independently through selection of contention window size and inter-frame space, leveraging the inherent unfairness of IEEE 802.11 to enhance the network's quality of service. Higher priority traffic is permitted (encouraged) to capture the channel from lower priority traffic flows.

Similar results can be achieved by four instances of the distributed algorithm, each computing the allocation for a single access category. Prioritization is achieved through dynamic coordination of the four auction capacities at each node. A potential strategy sets the capacity for each access category equal to one minus the allocation to higher priority access categories. As a result, higher priority auctions are permitted to starve lower priority auctions of capacity, effectively distributing channel access to high priority traffic. Alternatively, auction capacities can be selected to ensure a minimum or maximum percentage of the channel is offered to an access category. Although traffic within an access category follows the lexicographic max-min allocation, bidder's can weight their claims to prioritize traffic *within* the access category.

A network can run multiple instances of the distributed algorithm. For example, an instance of the Physical Receivers configuration with all demands set to one can be run concurrently with four instances configured to support differentiated service.

VII. RELATED WORK

This paper focuses on the topology and load-aware (TLA) allocation, its continuous distributed computation, and its application to transmitter persistences in wireless networks. In this section, we review a representative set of wireless MAC protocols, observing how each selects a node's persistence.

One class of protocol implements fixed persistences. A simple example is persistent CSMA [33] which employs persistences directly, transmitting in a given slot with probability p and deferring with probability $1 - p$. Scheduled MACs also implement persistences. Any finite schedule used in a cyclically repeated way can be generalized as a (k, v) -schedule with k transmission slots per frame of v slots, producing an effective persistence of $p = k/v$. Examples include the random schedules of [6], [24] where each node selects its k transmission slots randomly from the set of v slots in the frame. The fixed schedules of TDMA assign exactly one slot to each transmitter ($k = 1$) per frame ($v = \text{number of nodes}$). Topology transparent schemes [4], [19], [31] also implement (k, v) -schedules, offering more than one transmission opportunity ($k > 1$) per frame. The combinatorial requirements for variable weight topology transparent schedules (variable k) are explored in [25]; their construction remains an open problem.

The persistences of (k, v) -schedules are limited to v discrete values in the range $[0, 1]$. The periodic slot chains proposed in [18] are not limited to the structure of a fixed length frame

and can support arbitrarily precise persistences. A slot chain is defined by its starting transmission slot and period between its consecutive transmission slots. The persistence of a slot chain is the inverse of its period. By combining multiple slot chains with different periods, schedules are constructed targeting any rational persistence in the range $[0, 1]$.

Other MAC protocols compute schedules dynamically. Examples are FRPR [36] and CATA [34] which alternate between contention and scheduled phases; the contention phases compute new schedules, each with an implicit persistence, to accommodate network topology and traffic demands. SEEDEX [29] adjusts persistences dynamically as well, but only to accommodate network topology. It computes a persistence for each slot, deriving a node's probability to transmit from the number and identity of adjacent nodes.

Perhaps most prevalent is the class of contention-based MAC protocols. ALOHA [2], a simple contention-based MAC, transmits a message whenever there is one to send. If unsuccessful, it waits a random amount of time before retransmitting. Other schemes build on ALOHA by incorporating control messaging or revising the back-off mechanism for retransmissions. Various control messages have been proposed. Ready to Send (RTS) and Clear to Send (CTS) messages are used by MACA [20], MACAW [3], and IEEE 802.11 [15]. The latter two also implement per packet acknowledgements. Ready to Receive (RTR) messages are used by the receiver initiated protocols MACA-BI [32], RIMA-SP and RIMA-DP [10]. Negative acknowledgements are employed in [30]. Binary exponential back-off (BEB) is used by IEEE 802.3 [14] and IEEE 802.11 [15] to control the size of the contention window from which retransmit times are selected. Alternate back-off schemes have been considered, e.g., MILD [3], LMILD [7], SBA [12], and FAMA-NTR [9]. Regardless of back-off scheme or control messaging used, contention-based MACs determine each transmission's *instantaneous persistence*,

$$\frac{\text{Transmit Time}}{\text{MAC Latency} + \text{Transmit Time}}$$

where Transmit Time is the time required to transmit the packet and MAC Latency is the time the packet spends queued at the MAC layer. Although instantaneous persistences can vary drastically, their average is the long-term persistence of their transmitter. Both forms of persistence are artifacts of the back-off mechanism and control messaging employed.

The protocols outlined here focus on specific MAC challenges such as collision avoidance, spatial reuse, or minimization of delay. A different approach is taken in our earlier work [26] where the *topological allocation* is proposed as an ideal set of persistences for a given topology and traffic load. A distributed algorithm for computing the allocation is provided however it has several limitations [26]: (1) The algorithm assumes a priori knowledge of traffic demands and local topology. (2) It does not accommodate changes in topology or traffic demands. (3) The algorithm relies on strict synchronization requiring simultaneous initialization of bidders and auctioneers. The distributed algorithm proposed in this paper and employed by ATLAS solves these limitations by asynchronously adapting to changes in both topology and

traffic demand.

VIII. CONCLUSION

In our previous work [26], we define the TLA allocation and propose its use as a target allocation goal for transmitter persistences in a wireless network. The necessity for a decentralized and adaptive computation of the allocation has been an obstacle to its use in real world networks. In this paper, we give a distributed auction-based algorithm that converges continuously on the TLA allocation, adapting to changes in both topology and traffic load. The utility of the algorithm is demonstrated through integration into ATLAS which we simulate under a wide variety of network settings and scenarios. The new MAC performs well in mobile networks and provides MAC layer services supporting multi-hop TCP. It remains to be seen how ATLAS handles a more realistic physical medium where transmitters interfere beyond the range of their transmissions and asymmetric communication is common. Nevertheless, the body of results presented here suggests that the distributed algorithm, when employed at the wireless MAC layer, can effectively inform the selection of transmitter persistences, enabling a simple MAC protocol to provide robust, reliable, and scalable services. The application of the distributed algorithm is not restricted to the computation of transmitter persistences. It has the potential to inform routing and admission control decisions and to enable differentiation of service at the MAC layer. In this context, the algorithm provides a potential solution to the immediate challenge of medium access control, but also shows promise as a tool for use in network protocol design in general.

REFERENCES

- [1] *RFC 1323: TCP Extensions for High Performance*, 1992.
- [2] N. Abramson. The ALOHA system - Another alternative for computer communications. In *Proceedings of the Fall Joint Computer Conference*, pages 281–285, 1970.
- [3] V. Bharghavan, A. Demers, S. Shenker, and L. Zhang. MACAW: A medium access protocol for wireless LANs. In *Proceedings of the ACM Conference on Communications Architectures, Protocols and Applications (SIGCOMM'94)*, pages 212–225, London, UK, 1994.
- [4] I. Chlamtac and A. Faragó. Making transmission schedules immune to topology changes in multi-hop packet radio networks. *IEEE/ACM Transactions on Networking*, 2(1):23–29, February 1994.
- [5] I. Chlamtac and S. S. Pinter. Distributed nodes organization algorithm for channel access in a multihop dynamic radio network. *IEEE Transactions on Computers*, C-36(6):728–737, June 1987.
- [6] C. J. Colbourn and V. R. Syrotiuk. Scheduled persistence for medium access control in sensor networks. In *Proceedings from the First IEEE International Conference on Mobile Ad hoc and Sensor Systems (MASS'04)*, pages 264–273, Fort Lauderdale, Florida, USA, October 2004.
- [7] J. Deng, P. K. Varshney, and J. Haas. A new backoff algorithm for the IEEE 802.11 distributed coordination function. In *Proceedings of Communication Networks and Distributed Systems Modeling and Simulations (CNDS'04)*, January 2004.
- [8] L. C. Freeman. A set of measures of centrality based on betweenness. *Sociometry*, 40(1):35–41, 1977.
- [9] C. L. Fullmer and J. Garcia-Luna-Aceves. Floor acquisition multiple access (FAMA) for packet-radio networks. In *Proceedings of the Conference on Applications, Technologies, Architectures, and Protocols for Computer Communication, (SIGCOMM'95)*, volume 25, pages 262–273, Cambridge, Massachusetts, USA, 1995.
- [10] J. Garcia-Luna-Aceves and A. Tzamaloukas. Receiver-initiated collision avoidance in wireless networks. *Wireless Networks*, 8:249–263, 2002.

- [11] M. Gerla, R. Bagrodia, L. Zhang, K. Tang, and L. Wang. TCP over wireless multi-hop protocols: Simulation and experiments. In *Proceedings of the 1999 IEEE International Conference on Communication (ICC'99)*, pages 1089–1094, Vancouver, BC, Canada, June 1999.
- [12] Z. Haas and J. Deng. On optimizing the backoff interval for random access schemes. *IEEE Transactions on Communications*, 51(12):2081–2090, December 2003.
- [13] J. Hastad, T. Leighton, and B. Rogoff. Analysis of backoff protocols for multiple access channels. In *Proceedings of the 19th annual ACM Symposium on Theory of Computing (STOC'87)*, pages 740–744, New York, New York, USA, May 1987.
- [14] IEEE. *IEEE 802.3, CSMA/CD Ethernet access method*, 1983.
- [15] IEEE. *IEEE 802.11, Wireless LAN medium access control (MAC) and physical layer (PHY) specifications*, 1997.
- [16] IEEE. *IEEE 802.11e, Enhancements: QoS, including packet bursting*, 2007.
- [17] J. Boleng, N. Bauer, T. Camp, and W. Navidi. Random Waypoint Steady State Mobility Generator (mobgen-ss). <http://toilers.mines.edu/>.
- [18] G. Jakllari, M. Neufeld, and R. Ramanathan. A framework for frameless TDMA using slot chains. In *Proceedings of the 9th IEEE International Conference on Mobile Ad hoc and Sensor Systems (MASS'12)*, Las Vegas, Nevada, USA, October 2012.
- [19] J. Ju and V. O. K. Li. An optimal topology-transparent scheduling method in multihop packet radio networks. *IEEE/ACM Transactions on Networking*, 6(3):298–305, June 1998.
- [20] P. Karn. MACA - a new channel access method for packet radio. In *Proceedings from the ARRL/CRRL Amateur Radio 9th Computer Networking Conference*, pages 134–140, 1990.
- [21] V. Kawadia and P. R. Kumar. Experimental investigations into TCP performance over wireless multihop networks. In *Proceedings of the 2005 ACM SIGCOMM workshop on Experimental approaches to wireless network design and analysis (E-WIND'05)*, pages 29–34, Philadelphia, Pennsylvania, USA, August 2005.
- [22] D. Koutsonikolas, J. Dyaberi, P. Garimella, S. Fahmy, and Y. C. Hu. On TCP throughput and window size in a multihop wireless network testbed. In *Proceedings of the 2nd ACM International Workshop on Wireless network testbeds, experimental evaluation and characterization (WiNTECH'07)*, Montréal, Québec, Canada, September 2007.
- [23] K. Leung and V. O. K. Li. Transmission control protocol (TCP) in wireless networks: Issues, approaches, and challenges. *IEEE Communications Surveys & Tutorials*, 8:64–79, 2006.
- [24] J. Lutz, C. J. Colbourn, and V. R. Syrotiuk. Apples and oranges: Comparing schedule- and contention-based medium access control. In *Proceedings of the 13th ACM International Conference on Modeling, Analysis and Simulation of Wireless and Mobile Systems (MSWiM'10)*, pages 319–326, Bodrum, Turkey, October 2010.
- [25] J. Lutz, C. J. Colbourn, and V. R. Syrotiuk. Variable weight sequences for adaptive scheduled access in MANETs. In *Lecture Notes in Computer Science*, volume 7280, pages 53–64, 2012.
- [26] J. Lutz, C. J. Colbourn, and V. R. Syrotiuk. Topological persistence for medium access control. *IEEE Transactions on Mobile Computing*, to appear.
- [27] The Network Simulator ns-2. <http://www.isi.edu/nsnam/ns/>.
- [28] M. Pióro and D. Medhi. *Routing, Flow, and Capacity Design in Communication and Computer Networks*. Elsevier Inc., 2004.
- [29] R. Rozovsky and P. R. Kumar. SEEDEX: A MAC protocol for ad hoc networks. In *Proceedings of the 2nd ACM International Symposium on Mobile Ad Hoc Networking and Computing (MobiHoc'01)*, pages 67–75, Long Beach, California, USA, October 2001.
- [30] J. L. Sobrinho and A. S. Krishnakumar. Distributed multiple access procedures to provide voice communications over IEEE 802.11 wireless networks. In *Proceedings of the Global Telecommunications Conference, (GlobeCom'96)*, volume 3, pages 1689–1694, London, UK, November 1996.
- [31] V. R. Syrotiuk, C. J. Colbourn, and S. Yellamraju. Rateless forward error correction for topology-transparent scheduling. *IEEE/ACM Transactions on Networking*, 16(2):464–472, 2008.
- [32] F. Talucci, M. Gerla, and L. Fratta. MACA-BI (MACA by invitation) – a receiver oriented access protocol for wireless multihop networks. In *Proceedings of the IEEE 6th International Conference on Universal Personal Communications Record*, volume 2, pages 913–917, San Diego, California, USA, October 1997.
- [33] A. S. Tanenbaum. *Computer Networks*. McGraw Hill, fourth edition, 2003.
- [34] Z. Tang and J. Garcia-Luna-Aceves. A protocol for topology-dependent transmission scheduling in wireless networks. In *Proceedings*

of the IEEE Wireless Communications and Networking Conference, (WCNC'99), pages 1333–1337, 1999.

- [35] Y. Tian, K. Xu, and N. Ansari. TCP in wireless environments: Problems and solutions. *IEEE Communications Magazine*, 43:27–32, 2005.
- [36] C. Zhu and M. S. Corson. A five-phase reservation protocol (FPRP) for mobile ad hoc networks. *Wireless Networks*, 7(4):371–384, 2001.

PLACE
PHOTO
HERE

Jonathan Lutz earned his B.S. in Electrical Engineering from Arizona State University, Tempe, Arizona, in 2000 and his M.S. in Computer Engineering from the University of Waterloo, Waterloo, Canada, in 2003. He is currently working on his Ph.D. in Computer Science at Arizona State University. His research interests include medium access control in mobile ad hoc networks.

PLACE
PHOTO
HERE

Charles J. Colbourn earned his Ph.D. in 1980 from the University of Toronto, and is a Professor of Computer Science and Engineering at Arizona State University. He is the author of *The Combinatorics of Network Reliability* (Oxford), *Triple Systems* (Oxford), and 320 refereed journal papers focussing on combinatorial designs and graphs with applications in networking, computing, and communications. In 2004, he was awarded the Euler Medal for Lifetime Research Achievement by the Institute for Combinatorics and its Applications.

PLACE
PHOTO
HERE

Violet R. Syrotiuk earned her Ph.D. in Computer Science from the University of Waterloo (Canada). She is an Associate Professor of Computer Science and Engineering at Arizona State University. Her research has been supported by grants from NSF, ONR, and DSTO, and contracts with LANL, Raytheon, General Dynamics, and ATC. She serves on the editorial boards of *Computer Networks* and *Computer Communications*, as well as on the technical program and organizing committees of several major conferences sponsored by ACM and IEEE.